RSC Advances

PAPER

View Article Online
View Journal | View Issue

Cite this: *RSC Adv.*, 2020, **10**, 28422

Through bond energy transfer (TBET)-operated fluoride ion sensing *via* spirolactam ring opening of a coumarin–fluorescein bichromophoric dyad†

Subrata Kumar Padhan,[a] Vipin Kumar Mishra,[b] Narayan Murmu,[a] Sabyashachi Mishra *[b] and Satya Narayan Sahu *[a]

Received 18th June 2020
Accepted 24th July 2020

DOI: 10.1039/d0ra05357k

rsc.li/rsc-advances

The detection of fluoride ions in a competitive environment often poses several challenges. In this work, we have designed and synthesized a coumarin functionalized fluorescein dyad (**R3**) which represents an ideal through bond energy transfer (TBET) fluorophore with the coumarin unit as donor and fluorescein unit as acceptor. The bichromophoric dyad demonstrates the detection of fluoride ions in the parts per billion (ppb) concentration level (22.8 ppb) with high selectivity *via* a TBET emission signal at 548 nm with a diagnostic bright yellow colour fluorescence output. Based on UV-visible, fluorescence, ^{1}H NMR and DFT studies, it is shown that the fluoride ion induces the opening of the spirolactam ring of the fluorescein moiety and provides a π-conjugation link between the donor and acceptor units enabling a TBET phenomenon with a larger pseudo-Stokes shift of 172 nm. To the best of our knowledge, this is the first report where the fluoride ion is detected *via* a TBET signal between the coumarin and fluorescein units in a bichromophoric dyad.

1. Introduction

Fluorides are one of the important anions owing to their unique chemical reactivity and important applications in the areas of environmental, biological, chemical and medical sciences.[1,2] For instance, at lower concentrations, fluoride can form strong hydrogen bonds with neutral hydrogen-bond donors while it becomes a very strong base to promote deprotonation through typical Brønsted acid–base reactions at higher concentrations.[3,4] Excess of fluoride ions in the human body can lead to dental and skeletal deformation while its deficiency can cause osteoporosis.[5,6] Therefore, the detection of fluoride ions with high selectivity and sensitivity has been one of the foremost research goals over the last few years.[7–9]

Among the various detection techniques, the fluorescence based approach is considered as one of the preferred methods because of its simplicity and high sensitivity which translates each molecular event into a distinct fluorescence output.[10–12] Several fluorescence based approaches, such as, photoinduced electron transfer (PET),[13] intramolecular charge transfer (ICT)[14] and excited state intramolecular proton transfer (ESIPT)[15–18] have been designed for detection of fluoride ions. However, these techniques suffer a serious drawback on the loss of fluorescence intensity of the output signal as the photophysical processes in the excited state and the fluorescence emission originates from a single fluorophore. Consequently, resonance energy transfer (RET) or electronic energy transfer (EET) phenomenon comes out as a successful technique where a molecule absorbs light at the donor wavelength and emits at a wavelength characteristic of the acceptor unit.[19–21] Further, this technique offers significant advantages over the other fluorescence based approaches on the basis of long wavelength emission band with large pseudo-Stokes shift and a fluorescence turn-on mode.[22] Thus, various scientific groups at the present time are taking a keen interest in the construction of donor–acceptor energy transfer cassettes.[23]

In principle, the mechanism of energy transfer between two chromophoric moieties (donor to acceptor) can take place either through space or through conjugated bonds. Accordingly, it generates two processes such as, fluorescence resonance energy transfer (FRET) and through bond energy transfer (TBET), where the excited state energy transfer occurs through space and through bond, respectively.[24] However, the design of a FRET system often requires a meticulous selection of a suitable combination of donor and acceptor moieties which are attached *via* a flexible non-conjugated linker with a prerequisite that the donor emission must overlap considerably with the acceptor absorption band to observe an energy transfer signal within a spatial distance of 10–100 Å.[25] In contrast, a TBET system can be achieved with a large variety of donor and acceptor combinations which can be linked electronically but nonplanarly *via* rigid conjugated bonds that facilitate the energy transfer from donor to acceptor unit without or with a minimum spectral overlap between the donor emission

[a]*School of Chemistry, Sambalpur University, Jyoti Vihar, Burla-768 019, Odisha, India. E-mail: snsahu.chem@gmail.com; snsahu@suniv.ac.in*

[b]*Department of Chemistry, Indian Institute of Technology, Kharagpur – 721302, India. E-mail: mishra@chem.iitkgp.ac.in*

† Electronic supplementary information (ESI) available. See DOI: 10.1039/d0ra05357k

and acceptor absorption bands.[26] Thus, developing a TBET based receptor carries significant advantages over FRET based receptors in terms of its higher energy transfer efficiency and larger pseudo-Stokes shift.[23] Among the various chromophoric groups, coumarin and fluorescein derivatives have been extensively employed to design fluorescent probes due to their higher molar absorptivity and quantum yield.[27–29] Although a number of articles have been published on the fluorogenic detection of fluoride ions,[30,31] to the best of our knowledge no report is available for fluoride sensing based on a TBET system. Therefore, it is envisaged that, suitable mounting of a coumarin and fluorescein unit on a single molecular framework could lead to a donor–acceptor system that can detect fluoride ions *via* TBET process.

With this vision, and in continuation to our efforts on the development of chromofluorogenic fluoride ion sensors,[32,33] we have designed and synthesized a coumarin functionalized fluorescein dyad (**R3**) in the present work. The bichromophoric dyad exhibits a highly selective sensing of fluoride ions amongst the other tested anions *via* TBET mechanism. The fluoride ion induces the opening of the spirolactam ring of the fluorescein moiety and thereby provides a π-conjugation link between the donor coumarin and the acceptor fluorescein, which subsequently exhibits the TBET phenomenon with a much larger pseudo-Stokes shift of 172 nm. Further, the dyad shows a stronger binding constant and ppb level of sensitivity toward fluoride ion. We believe that, this is the first report where fluoride induced-TBET signal is observed between coumarin and fluorescein units in a bichromophoric dyad system.

2. Results and discussion

2.1. Synthesis and characterization of dyad R3

The general experimental methods, preparation of test samples and synthetic procedure for compounds **1**, **2** and **R3** (Scheme 1) have been described in detail in the ESI.† The dyad **R3** was synthesised as per the synthetic protocol given in Scheme 1. The condensation reaction of fluorescein hydrazide (**2**) with 8-formyl-7-hydroxy-4-methyl coumarin in ethanolic medium under reflux condition for 8.0 hours afforded the compound **R3** in quantitative yield. The analytical characterization of **R3** was consistent with its indicated structure (Fig. S1–S4†). For example, ^{1}H NMR spectrum of **R3** (Fig. S1†) exhibits a singlet at δ 9.70 ppm which can be assigned to azomethene (–CH=N–) proton. The corresponding ^{13}C NMR signal of the azomethene carbon (–CH=N–) was appeared at 165.1 ppm which evidently supports the formation of a fluorescein conjugated Schiff base **R3** (Fig. S2†). The FTIR spectrum shows a strong band at 1620 cm^{-1} which corresponds to the C=N stretching frequency of the azomethene group (Fig. S3†). The ESI-MS data further confirmed the formation of **R3** by the appearance of a signal at m/z 533.02 for the $[M + H]^+$ ion (Fig. S4†).

2.2. Photophysical studies of dyad R3 with fluoride ions

The binding characteristics of compound **R3** was investigated toward different anions (F^-, Cl^-, Br^-, I^-, $H_2PO_4^-$, HSO_4^-, AcO^- as their tetrabutylammonium salts, CN^- as potassium salt and S^{2-} as sodium salt) by absorption and emission spectroscopy. Dyad **R3** (10 μM) exhibited a band at 326 nm due to the coumarin moiety, while there is no band corresponding to the fluorescein unit was observed in its UV-visible spectrum (Fig. S5a†). On gradual addition of fluoride ions (0–5 equiv.), the intensity at 326 nm band decreases with the appearance of new absorption bands at 375 and 524 nm and elicits a visual colour transformation from colourless to pink in the solution medium (Fig. S5a,† 1a and b). The newly emerged band at 375 nm could be attributed to the binding of fluoride ion with the coumarin hydroxyl group while the band at 524 nm is ascribed to the opening of spirolactam ring of fluorescein unit *via* fluoride ion binding at the fluorescein hydroxyl group.

Further, in order to check the interaction of fluoride ions individually with the coumarin and fluorescein components, UV-visible spectra were recorded by adding excess fluoride ions (10 equiv.) to a solution of coumarin hydrazide (**1**) and fluorescein hydrazide (**2**) in acetonitrile medium (10 μM). It was observed that both the components **1** and **2** independently exhibited absorption band at 388 and 515 nm respectively upon interaction with fluoride ions (Fig. S5b†), which is very close to the absorption bands at 375 nm and 524 nm of **R3** in presence of fluoride ions (Fig. S5a†). This clearly indicates that both coumarin and fluorescein units in **R3** are interacting with

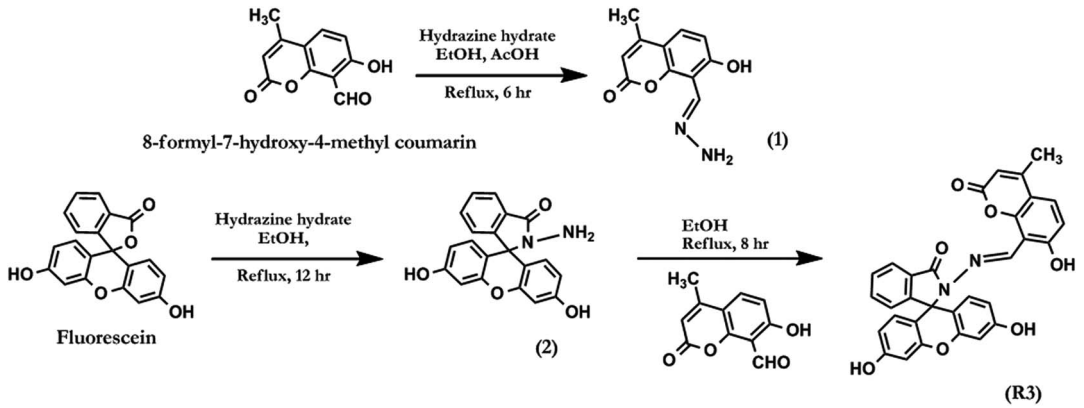

Scheme 1 Synthesis of dyad R3.

fluoride ions. However the molar absorption coefficient (ε) of **1** (ε_{388} = 21 400) is higher than that of **2** (ε_{515} = 1200) in the presence of fluoride ion.

On the other hand, in case of dyad **R3**, addition of fluoride ions exhibited an absorption spectrum comprising of both **1** and **2** components at 375 nm and 524 nm respectively with a higher molar absorption coefficient (ε_{524} = 52 700) value for fluorescein band in comparison to coumarin band (Fig. S5a†). This implies that a significant electronic interaction is operating between the coumarin and fluorescein (ring opened form) units in the ground state of **R3** by means of synergetic effect *via* π-conjugation. Consequently, the dyad can be employed for colorimetric sensing of fluoride ions with high selectivity (Fig. 1b).

In fluorescence study, the dyad **R3** shows a very weak emission band at 498 nm upon excitation between 325 to 400 nm which can be assigned to the signal of the coumarin moiety (inset of Fig. 2a). The possibility of electron transfer in the excited state (PET) from imino nitrogen to the coumarin fluorophore could be the reason behind the weak emissive nature of **R3**.[27,28] However, gradual addition of fluoride ions (0–5 equiv.) to the dyad solution (10 μM) resulted in emergence of an emission band at 548 nm upon excitation at 376 nm (Fig. 2a) with a pseudo-Stokes shift of 172 nm. Consequently, it turns on a diagnostic bright yellow fluorescence signal in the solution of **R3** in presence of fluoride ions under the UV-light at 365 nm (inset of Fig. 2b). This increase in the yellow fluorescence signal at 548 nm can be attributed to the opening of the spirolactam ring of fluorescein (amide form) on exposure to fluoride ions. On the other hand, when fluorescence studies were carried out by taking an equimolar mixture of coumarin component **1** and fluorescein component **2** with excess of fluoride ions (10 equiv.) in acetonitrile medium, a weak emission band at 500 nm with a shoulder at around 460 nm is appeared upon excitation on the coumarin absorption band at 376 nm (Fig. S6†).

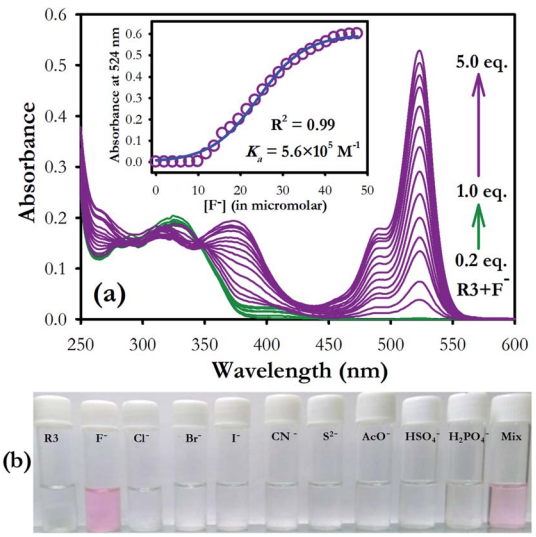

Fig. 1 (a) UV-visible titration spectra of dyad **R3** (10 μM in AcN) with 0–5.0 equiv. of TBAF. Inset shows the change in absorbance at 524 nm in the presence of various equivalents of F^- ions. (b) Colorimetric response of dyad **R3** (10 μM) in presence of 5.0 equiv. of various anions in AcN.

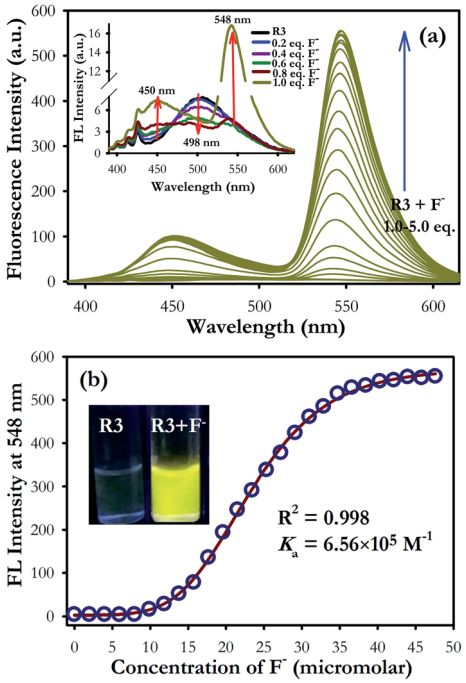

Fig. 2 (a) Fluorescence titration spectra of dyad **R3** (10 μM in AcN) upon addition of 0.0–5.0 equiv. of F^- ions and (b) shows change in fluorescence intensity at 548 nm with varying concentration of F^- ions. Inset of figure (a) shows zoomed fluorescence spectra of **R3** upon addition of 0.0–1.0 equiv. of F^- ions and inset of figure (b) shows the change in visual fluorescence colour in **R3** with the addition of fluoride ions.

Moreover, the fluorescence enhancement factor (I/I_0) of dyad **R3**, fluorescein component **2** (ring opened amide form) and equimolar coumarin–fluorescein pair (**1** + **2**) in presence of fluoride ions are 130, 19 and 29-fold respectively when excited at 376 nm (inset of Fig. S6†). This strongly indicates that a very fast intramolecular energy transfer is operating in dyad **R3** where coumarin unit performs the role of a donor while the ring opened form of fluorescein acts as the acceptor unit resulting in a TBET signal in the presence of fluoride ions. In contrast, there is a weak intermolecular energy transfer possibly exists between the donor coumarin and acceptor fluorescein (amide form) in the equimolar donor–acceptor mixed solution. This result evidently supports that fluoride interaction with **R3** opens the spirolactam ring of the fluorescein unit that creates a π-conjugated linkage with the donor coumarin moiety to facilitate a strong TBET event.

The fluorescence titration experiment of **R3** with various equivalents of fluoride ion shows a gradual increase in emission intensity at 450 nm upto the addition of one equivalent (Fig. 2 and inset of Fig. S7a†). On further addition of fluoride ions, the intensity of the emission band at 450 nm increases along with the TBET emission band at 548 nm. However, the intensity of 450 nm band got saturated at two equivalents of fluoride ions. Based on the titration profile (Fig. S7a†), a proposed binding mode of fluoride ions with **R3** is presented in Scheme 2.

On comprehensive analysis of the profile, it is very clear that the initial addition of fluoride ions (upto one equivalent) interact with the coumarin-hydroxyl group of dyad **R3** resulting

in a single emission signal at 450 nm for the species **A** (Scheme 2). Addition of more than one equivalent of fluoride ions (upto two equivalents) could lead to the formation of species like **D** and **E** *via* the intermediate **C** (Scheme 2 and Fig. S7a†), which is evident by the appearance of two emission bands at 450 nm and 548 nm. Beyond the addition of two equivalents fluoride ion, the band at 450 nm exhibited a fall in intensity while the intensity of TBET emission band at 548 nm continued to increase till four equivalents and finally get saturated (inset of Fig. S7a†). When we observe the trail of the TBET signal at 548 nm through a ratiometric plot (I_{548}/I_{450}) with different equivalents of fluoride ions (Fig. S7b†), it clearly demonstrates that, below one equivalent, the anion preferentially interacts with the coumarin hydroxyl group while up to two equivalents, the formation of equilibrated species **D** and **E** *via* **C** is taking place. After two equivalents, a complete TBET signal is generated on subsequent addition of fluoride ions due to the formation of a π-conjugated species **P** which is fully accomplished beyond four equivalents. This observation strongly implies a stepwise interaction of fluoride ions with the dyad molecule at the two binding sites (one at coumarin hydroxyl and other at fluorescein hydroxyl groups) resulting in an overall TBET signal as shown in Scheme 2. Moreover the fluorescence enhancement factor of **R3** is greater than the other reported fluorescence sensors for fluoride ions[7,34] and the pseudo-Stokes shift observed in **R3** in the presence of fluoride ion is much higher than the recently reported FRET based-fluoride ion sensor.[35] Besides, the fluoride ion induced fluorescence colour of dyad **R3** is much brighter and appears at higher wavelength region than the sole fluorescein acceptor (**2** in ring opened amide form) when observed under the UV lamp at 365 nm (inset of Fig. S6†). This indicates that the TBET signal of **R3** is much stronger than that of fluorescein acceptor signal without the coumarin donor when excited at the donor wavelength. Thus, the dyad can act as an excellent TBET-based sensor for detection of fluoride ions.

We have further examined the fluorescence response of **R3** with other anionic species such as Cl^-, Br^-, I^-, $H_2PO_4^-$, HSO_4^-, AcO^-, CN^- and S^{2-} ion. Addition of other anions to **R3** did not show any significant change in its emission signal thereby indicating a highly selective behavior of the dyad toward fluoride ions (Fig. 3). The competitive experiments of **R3** with fluoride ion (10 equiv.) in the presence of other anions (10 equiv. each) showed no substantial variation in the fluorescence intensity of the **R3**–F^- complex. This demonstrates the practical applicability of **R3** toward detection of fluoride ions along with other interfering species (Fig. 3a and b). The binding behavior of **R3** with fluoride ion is quantitatively analyzed by Job's plot which exhibited a maximum optical response at 0.33 mole fraction of the dyad to indicate a 1 : 2 stoichiometry between **R3** and F^- ions (Fig. S8†). The nonlinear fit of the measured absorbance at 524 nm *versus* various concentration of F^- ions in **R3** revealed a sigmoid relationship with a correlation (R^2) of 0.995 (inset of Fig. 1). The very high association constant (K_a) for **R3** (5.6×10^5 M^{-1}) indicated a higher binding affinity of this dyad toward F^- ions. Further, the binding constant for **R3** ($K_a = 6.56 \times 10^5$ M^{-1}) evaluated from fluorescence titration data (Fig. 2b) are well in line with those measured from UV-visible experiments. The dyad **R3** shows a limit of detection (LOD) of 2.6 μM (49.4 ppb) and 1.2 μM (22.8 ppb) by UV-visible and fluorescence experiments, respectively (Fig. S9†) which indicates a high level of sensitivity of the dyad toward F^- ion.

2.3. Proton NMR studies of dyad R3 with fluoride ions

The binding interaction of **R3** with fluoride ions was also investigated by proton NMR titration experiments in DMSO-d_6 at 5.0 mM concentration (Fig. 4). The dyad **R3** exhibits five singlets beyond the aromatic range at δ 11.57, 10.05, 9.70, 6.71 and 6.26 ppm in its NMR spectrum that could be assigned to hydroxyl group (–OH-1) of coumarin unit, hydroxyl group (–OH-2) of fluorescein unit and proton numbers H10, H3 and H11

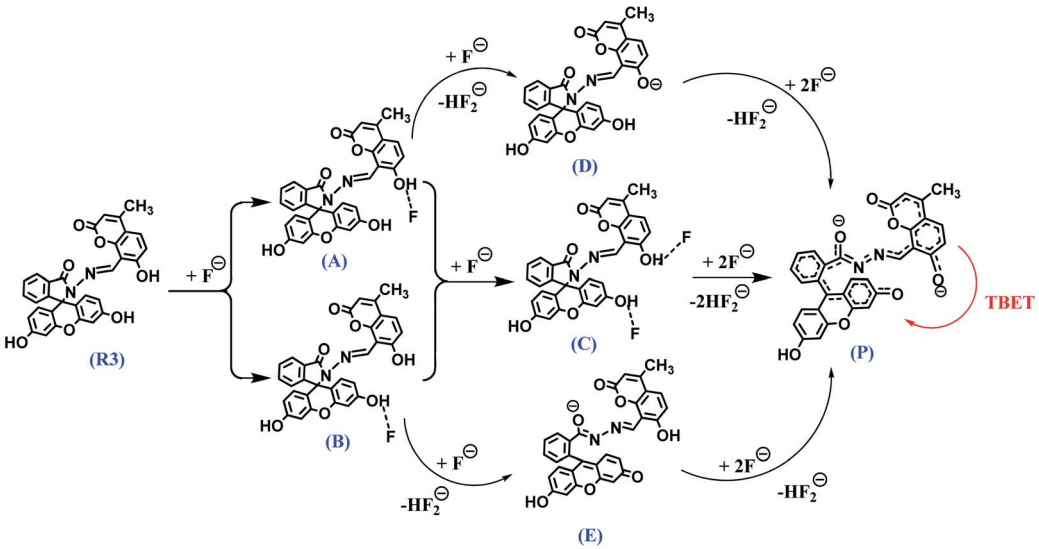

Scheme 2 A proposed binding mode and deprotonation of **R3** in the presence of fluoride ions and the resultant TBET phenomenon.

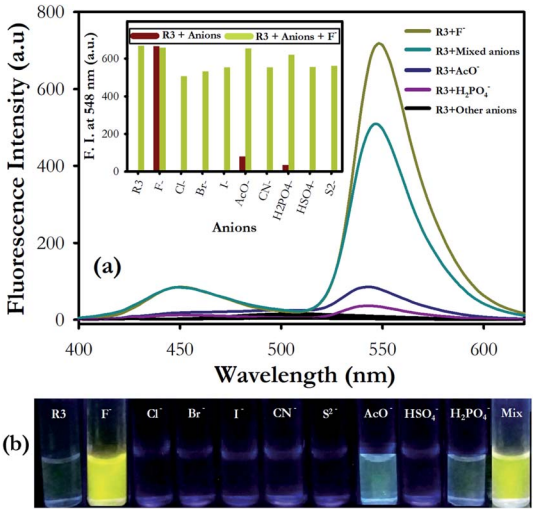

Fig. 3 (a) Emission spectra of dyad **R3** (10 μM in AcN) with 10.0 equivalents of various anions. Inset shows the fluorescence intensity of **R3** at 548 nm with 10.0 equivalents of various anions (red bar) and with 10.0 equivalents of various anions plus 10.0 equivalents F^- ions (green bar). (b) Visual fluorogenic response of **R3** with 10.0 equivalents of various anions under UV-lamp at 365 nm.

respectively. A significant change was observed in the chemical shift values of the proton signals upon the addition of 1.0 equivalent of fluoride ion to **R3.** For instance, the –OH signals at δ 11.57 and 10.05 ppm corresponding to hydroxyl groups (–OH-1 and OH-2) became broaden while the singlets at δ 9.70, 6.71 and 6.26 ppm corresponding to protons H10, H3 and H11 showed a marginal upfield shift in their positions. However, addition of 2.0 equivalents of fluoride ion further broadens the –OH signals which became indistinguishable subsequently. On the other hand, the H10 and H11 proton signals at δ 9.70 and 6.26 ppm, respectively exhibited further upfield shifts in their chemical shift values whereas other protons signals get blurred. Subsequent addition of fluoride ions (5.0 equiv.) exhibited complete disappearance of –OH signals while the proton signals corresponding to H10 and H11 showed an upfield shift of $\Delta\delta$ 0.81 ppm (from δ 9.70 to 8.89) and $\Delta\delta$ 0.59 ppm (from δ 6.26 to 5.67) respectively. On the other hand, the proton signal of H12 gets separated and appeared as a distinguishable signal at δ 7.24 ppm in the NMR spectrum at higher fluoride concentration.

Analysis of the NMR titration experiment indicates that the dyad forms a hydrogen bond adduct within one equivalent of fluoride ion as evident by the broadening of –OH signals at δ 11.57 and 10.05 ppm. Subsequent addition of fluoride ions caused complete disappearance of the –OH signals due to deprotonation which was confirmed by the appearance of a triplet at around δ 16 ppm, a signature signal for the formation of HF_2^- species on deprotonation as depicted in Scheme 2. This process of hydrogen bond formation of **R3** at lower equivalents of fluoride ion followed by deprotonation at higher equivalents was further established by the gradual upfield shifts of the signals corresponding to azomethene proton (–CH=N–)

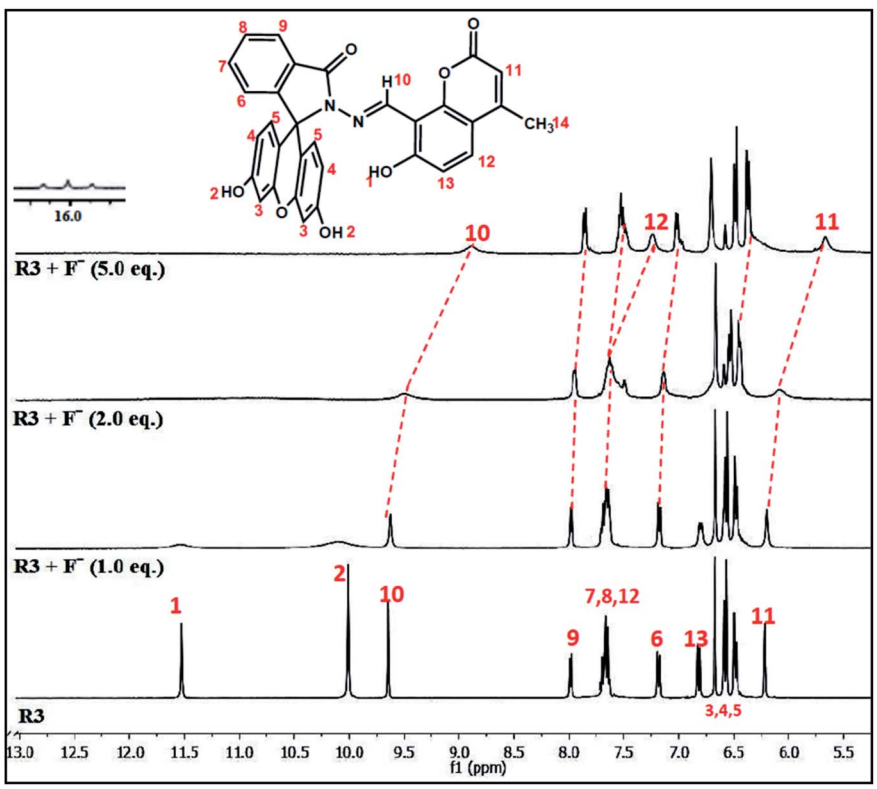

Fig. 4 ^{1}H NMR titration spectra of dyad **R3** (5.0 mM) upon addition of various equivalents of F^- ion in DMSO-d_6.

H10, coumarin protons (H11 and H12) and aromatic protons (H3 and H5) of the fluorescein unit arising due to increase of intramolecular charge transfer within the dyad. These observations suggest that, **R3** forms 1 : 1 hydrogen bonded complex with F^- ion upto one equivalent as indicated in structure **A** and **B** (Scheme 2) which cause a minimal change in its optical properties. However, upto two equivalents of fluoride ions, **R3** forms either a 1 : 2 (**R3** : fluoride) hydrogen-bond adduct **C** or partial deprotonated species like **D** or **E** as depicted in Scheme 2. Beyond four equivalents of fluoride ions, the dyad undergoes deprotonation of –OH protons forming the π-conjugated product **P** (Scheme 2) which strongly facilitates the TBET process.

2.4. DFT studies on interaction of dyad R3 with fluoride ions

To get a better perception of the optical properties of **R3** and its interaction with fluoride ions, quantum mechanical calculations were performed on model compounds by employing density functional theory (DFT) using CAM-B3LYP functional[36] and 6–311++G(d,p) basis set[37] in gas phase and in acetonitrile solvent (*via* a polarized continuum model) using Gaussian 09.[38] The dyad **R3**, its fluoride intermediates **A**, **B**, **C**, **D**, **E** and the deprotonated product **P** (Scheme 2 and Fig. S10†) were optimized and the optimized structures were further validated by carrying out Hessian calculations, where all vibrational frequencies were found to be positive. The mechanism of interaction of **R3** with fluoride ion is deduced by analyzing the electron density distribution in the frontier molecular orbitals HOMO (highest occupied molecular orbital) and LUMO (lowest unoccupied molecular orbital) of the studied system as shown in Fig. 5. The electron distribution both in HOMO and LUMO of dyad **R3** are delocalized over the entire molecule, whereas the HOMO and LUMO of the product **P** are exclusively populated on the coumarin donor and the fluorescein acceptor parts, respectively (Fig. 5).

With reference to the energy (in kcal mol^{-1}) of the free dyad **R3**, the optimized energy of the intermediates **A** (−19.0), **B** (−16.1), **C** (−33.9), **D** (−26.6), **E** (−4.3) and the product **P** (−25.9) were found to be lower, which signifies a better stability of the intermediates and product (Fig. S10 and Table S1†). The HOMO energy levels of the fluoride complexes are found to be higher than that of the free dyad molecule (Fig. 5) which can be attributed to the stabilizing interaction of the electron in the dyad **R3** where the HOMO is delocalized over the entire molecule, thus providing lower orbital energy. In contrast, the calculated HOMO and LUMO energy gap (in eV) of the dyad is larger than that of the intermediates (**A**, **B**, **C**, **D** and **E**) and the product **P** (Fig. 5), which corroborates the red shifts observed in the UV-visible spectra of **R3** upon the addition of F^- ions.

Moreover, upon comparison of the relative energy of two types of 1 : 1 fluoride complexes **A** and **B** (Scheme 2) with respect to free dyad **R3**, it is interesting to note that the species **A** is more stable than **B** (Table S1†). Similarly, addition of second equivalent of fluoride ion to **R3** resulting in a 1 : 2 fluoride complex **C** more preferably over the partial deprotonated species **D** and **E** due to its greater stability over the intermediates **D** and **E** (Table S1†). These results clearly imply that the hydrogen bonded adducts **A**, **B** and **C** are formed when the dyad **R3** interacts with fluoride ions up to two equivalents. On the other hand, it leads to a completely deprotonated species **P**

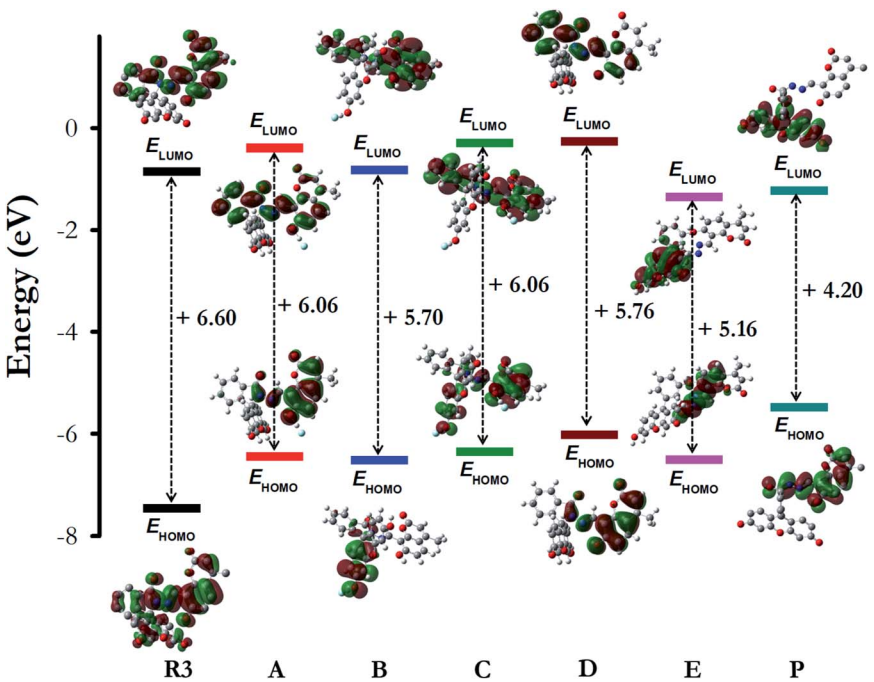

Fig. 5 The shape and energy of the HOMO and LUMO of dyad **R3**, intermediates (**A**, **B**, **C**, **D** and **E**) and product **P** calculated with DFT (CAM-B3LYP)/6–311++G(d,p) method (in acetonitrile solvent phase).

through the intermediate **D** beyond four equivalents of fluoride ions, as proposed in Scheme 2.

Based on the DFT studies and relative energy calculations, we have proposed a stepwise route of fluoride interaction with dyad **R3** as per Scheme 2. This route starts with the formation of an intermediate **A** initially with one equivalent of fluoride ion followed by intermediate **C** with two equivalents. Addition of fluoride ions beyond two equivalents leads to the formation of partial deprotonated intermediate **D** (more preferably over **E**) that subsequently generates the product **P** after four equivalents of fluoride ions. This putative route is also in concordance with the fluorescence studies and ^{1}H NMR experiments. For instance, one equivalent of fluoride ion preferably binds to the hydroxyl group of the coumarin donor which exhibits an emission signal at 450 nm and beyond that the second equivalent of fluoride ion binds to the hydroxyl group of fluorescein unit giving rise to fluorescence output at 548 nm. On further addition of fluoride ions (beyond 4 equiv.), there is formation of a π-conjugated species **P** which represents a perfect donor–acceptor pair to facilitate the through bond energy transfer as observed in the DFT studies (Fig. 6).

The electronic absorption and emission processes were further investigated by using time-dependent density functional theory (TD-DFT) calculations for the dyad **R3** and the product **P**. The calculated absorption bands, the corresponding oscillator strength (*f*), as well as the electronic transitions responsible for the absorption bands are summarized in Table S2.† The TD-DFT calculations predict absorption bands between 280–297 nm and 326–491 nm, for **R3** and product **P** (Scheme 2), respectively. The molecular orbitals corresponding to these states (for **R3** and product **P**) are shown in Fig. S11 and S12.† In case of product **P**, after photo-absorption, the system eventually relaxes to the equilibrium geometry of S_1 state from which the emission occurs to S_0 state. The S_1–S_0 emission is calculated to occur at 492 nm, which is in a qualitative agreement with the emission band observed in the experiment (548 nm). The electronic transition responsible for this emission band clearly shows that the emission band is associated with the electronic transition from the coumarin donor to the fluorescein acceptor of the product **P** (Fig. 6).

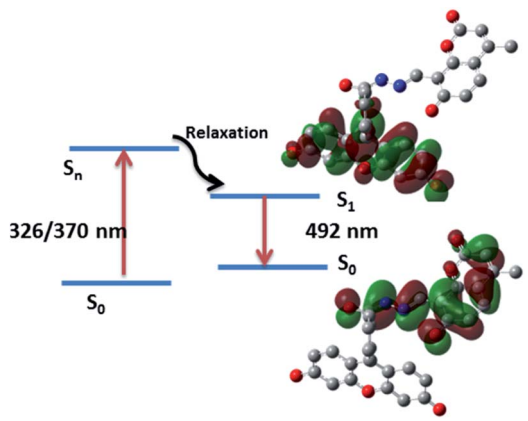

Fig. 6 Proposed TBET phenomenon in the deprotonated dyad **P**. The absorption (from S_0 to S_n) occurs at 326 to 370 nm. The system eventually relaxes to the equilibrium geometry of S_1 state from which the emission occurs to S_0 state at 492 nm.

3. Conclusions

In summary, we have designed and successfully synthesized a bichromophoric dyad (**R3**) which represents an ideal TBET system having coumarin as donor and fluorescein as acceptor fluorophore. This dyad demonstrates a highly selective detection of fluoride ions over other competitive anions through a TBET emission band at 548 nm along with a diagnostic yellow colour fluorescence output in the presence of fluoride ions. A careful analysis of the fluorescence titration experiment of dyad **R3** with fluoride ions revealed a step wise hydrogen bonding interaction of the anion at the two binding sites of the molecule, one at the coumarin hydroxyl group and the other at the fluorescein hydroxyl group. The fluoride ion initially interacts with the coumarin hydroxyl group within one equivalent while at higher equivalents it interacts with the fluorescein hydroxyl unit and subsequently generates the TBET signal as proposed in Scheme 2. The results of the fluorescence titration experiments are further corroborated with the proton NMR experiments and DFT studies, which evidently support the stepwise interaction of fluoride ion with the dyad molecule from lower to higher concentrations. The competitive experiment with other anions shows an extreme selectivity of dyad **R3** toward fluoride ions. Further, the dyad exhibits a ppb level of sensitivity for fluoride ion with a LOD of 49.4 ppb (2.6 μM) and 22.8 ppb (1.2 μM) by UV-visible and fluorescence method respectively. All together, these results could pave the way toward the development of molecular indicators for sensing fluoride ions in chemical and biological platforms.

Conflicts of interest

There are no conflicts to declare.

Acknowledgements

S. N. S gratefully acknowledges the financial assistance received from S&T Department, Govt. of Odisha for the research grant. The research grant received from GNM Foundation for Prof. G. N. Mahapatra Endowment Chair award is gratefully acknowledged. S. K. P. is thankful to DST and UGC New Delhi for a project assistantship and BSR fellowship respectively. N. M. is grateful to S&T Department, Govt. of Odisha for a project fellowship. V. K. M. acknowledges UGC, India for financial assistance. S. M. acknowledges the research grants from SERB, Govt. of India (EMR/2015/001890), DST-FIST, Govt. of India (SR/FST/CSII-026/2013), and CSIR, New-Delhi, India (01(2987)/19/EMR-II). Authors are thankful to Central Instruments Facility, NIT Rourkela and Materials Research Centre, MNIT Jaipur for recording the NMR and Mass spectra respectively. The financial assistance received by the School of Chemistry from UGC and DST New Delhi through the DRS and FIST grants, respectively, is gratefully acknowledged. We are thankful to Dr H. Chakraborty,

Sambalpur University for his useful suggestions toward the improvement of this manuscript.

References

1 C. Caltagirone and P. A. Gale, Anion receptor chemistry: highlights from 2007, *Chem. Soc. Rev.*, 2009, **38**, 520–563.
2 A. Bianchi, K. Bowman-James and E. Garcia-Espana, *Supramolecular Chemistry of Anions*, Wiley-VCH, New York, 1997.
3 H. M. Chawla, R. Shrivastava and S. N. Sahu, A new class of functionalized calix[4]arenes as neutral receptors for colorimetric detection of fluoride ions, *New J. Chem.*, 2008, **32**, 1999–2005.
4 V. Amendola, M. Boiocchi, L. Fabbrizzi and A. Palchetti, What anions do inside a receptor's cavity: a trifurcate anion receptor providing both electrostatic and hydrogen-bonding interactions, *Chem.–Eur. J.*, 2005, **11**, 5648–5660.
5 M. Kleerekoper, The role of fluoride in the prevention of osteoporosis, *Endocrinol. Metab. Clin. North Am.*, 1998, **27**, 441–452.
6 K. L. Kirk, *Biochemistry of the halogens and inorganic halides*, Plenum Press, New York, 1991.
7 Y. Zhou, J. F. Zhang and J. Yoon, Fluorescence and colorimetric chemosensors for fluoride-ion detection, *Chem. Rev.*, 2014, **114**, 5511–5571.
8 M. Cametti and K. Rissanen, Highlights on contemporary recognition and sensing of fluoride anion in solution and in the solid state, *Chem. Soc. Rev.*, 2013, **42**, 2016–2038.
9 M. Cametti and K. Rissanen, Recognition and sensing of fluoride anion, *Chem. Commun.*, 2009, **20**, 2809–2829.
10 J. R. Lakowicz, *Principles of fluorescence spectroscopy*, Springer, New York, 2007.
11 A. P. Demchenko, *Introduction to fluorescence sensing*, Springer, Dordrecht-Netherlands, 2009.
12 A. Dhillon, M. Nair and D. Kumar, Analytical methods for determination and sensing of fluoride in biotic and abiotic sources: a review, *Anal. Methods*, 2016, **8**, 5338–5352.
13 T. Gunnlaugsson, H. D. P. Ali, M. Glynn, P. E. Kruger, G. M. Hussey, F. M. Pfeffer, C. M. G. dos Santos and J. Tierney, Fluorescent photoinduced electron transfer (PET) sensors for anions; from design to potential application, *J. Fluoresc.*, 2005, **15**, 287–299.
14 L. Gai, J. Mack, H. Lu, T. Nyokong, Z. Li, N. Kobayashi and Z. Shen, Organosilicon compounds as fluorescent chemosensors for fluoride anion recognition, *Coord. Chem. Rev.*, 2015, **285**, 24–51.
15 X. Peng, Y. Wu, J. Fan, M. Tian and K. Han, Colorimetric and ratiometric fluorescence sensing of fluoride: tuning selectivity in proton transfer, *J. Org. Chem.*, 2005, **70**, 10524–10531.
16 Y. Wu, X. Peng, J. Fan, S. Gao, M. Tian, J. Zhao and S. Sun, Fluorescence sensing of anions based on inhibition of excited-state intramolecular proton transfer, *J. Org. Chem.*, 2007, **72**, 62–70.
17 K. Dhanunjayarao, V. Mukundama and K. Venkatasubbaiah, A highly selective ratiometric detection of F^- based on excited-state intramolecular proton-transfer (imidazole) materials, *J. Mater. Chem. C*, 2014, **2**, 8599–8606.
18 H. Dong, J. Zhao, H. Yang and Y. Zheng, The mechanism of ratiometric fluoride sensing and the ESIPT process for 2,6-dibenzothiazolylphenol and its derivative, *Org. Chem. Front.*, 2018, **5**, 1241–1247.
19 S. Speiser, Photophysics and mechanisms of intramolecular electronic energy transfer in bichromophoric molecular systems: solution and supersonic jet studies, *Chem. Rev.*, 1996, **96**, 1953–1976.
20 B. Albinsson and J. Mårtensson, Excitation energy transfer in donor-bridge-acceptor systems, *Phys. Chem. Chem. Phys.*, 2010, **12**, 7338–7351.
21 G. A. Jones and D. S. Bradshaw, Resonance energy transfer: from fundamental theory to recent applications, *Front. Physiol.*, 2019, **7**, 100.
22 N. Kumar, V. Bhalla and M. Kumar, Resonance energy transfer-based fluorescent probes for Hg^{2+}, Cu^{2+} and Fe^{2+}/Fe^{3+} ions, *Analyst*, 2014, **139**, 543–558.
23 J. Fan, M. Hu, P. Zhan and X. Peng, Energy transfer cassettes based on organic fluorophores: construction and applications in ratiometric sensing, *Chem. Soc. Rev.*, 2013, **42**, 29–43.
24 R. Zhang, F. Yan, Y. Huang, D. Kong, Q. Ye, J. Xu and L. Chen, Rhodamine-based ratiometric fluorescent probes based on excitation energy transfer mechanisms: construction and applications in ratiometric sensing, *RSC Adv.*, 2016, **6**, 50732–50760.
25 I. Medintz and N. Hildebrandt, *FRET-Forster Resonance Energy Transfer: From Theory to Applications*, Wiley-VCH, Weinheim, 2014.
26 W. Lin, L. Yuan, Z. Cao, Y. Feng and J. Song, Through-bond energy transfer cassettes with minimal spectral overlap between the donor emission and acceptor absorption: coumarin–rhodamine dyads with large pseudo-stokes shifts and emission shifts, *Angew. Chem., Int. Ed. Engl.*, 2010, **49**, 375–379.
27 D. Cao, Z. Liu, P. Verwilst, S. Koo, P. Jangili, J. S. Kim and W. Lin, Coumarin-based small-molecule fluorescent chemosensors, *Chem. Rev.*, 2019, **119**, 10403–10519.
28 X. Sun, T. Liu, J. Sun and X. Wang, Synthesis and application of coumarin fluorescence probes, *RSC Adv.*, 2020, **10**, 10826–10847.
29 F. Yan, K. Fan, Z. Bai, R. Zhang, F. Zu, J. Xu and X. Li, Fluorescein applications as fluorescent probes for the detection of analytes, *TrAC, Trends Anal. Chem.*, 2017, **97**, 15–35.
30 D. Udhayakumari, Detection of toxic fluoride ion *via* chromogenic and fluorogenic sensing. a comprehensive review of the year 2015–2019, *Spectrochim. Acta, Part A*, 2020, **228**, 117817.
31 P. Chen, W. Bai and Y. Bao, Fluorescent chemodosimeters for fluoride ions via silicon-fluorine chemistry: 20 years of progress, *J. Mater. Chem. C*, 2019, **7**, 11731–11746.

32 S. N. Sahu, S. K. Padhan and P. K. Sahu, Coumarin functionalized thiocarbonohydrazones as a new class of chromofluorescent receptors for selective detection of fluoride ion, *RSC Adv.*, 2016, **6**, 90322–90330.

33 S. K. Padhan, M. B. Podh, P. K. Sahu and S. N. Sahu, Optical discrimination of fluoride and cyanide ions by coumarin–salicylidene based chromofluorescent probes in organic and aqueous medium, *Sens. Actuators, B*, 2018, **255**, 1376–1390.

34 S. Dhiman, M. Ahmad, N. Singla, G. Kumar, P. Singh, V. Luxami, N. Kaur and S. Kumar, Chemodosimeters for optical detection of fluoride anion, *Coord. Chem. Rev.*, 2020, **405**, 213138.

35 B. Qiu, Y. Zeng, R. Hu, L. Chen, J. Chen, T. Yu, G. Yang and Y. Li, Förster resonance energy-transfer-based ratiometric fluorescent indicator for quantifying fluoride ion in water and toothpaste, *ACS Omega*, 2018, **3**, 18153–18159.

36 T. Yanai, D. P. Tew and N. C. Handy, A new hybrid exchange–correlation functional using the Coulomb-attenuating method (CAM-B3LYP), *Chem. Phys. Lett.*, 2004, **393**, 51–57.

37 R. Ditchfield, W. J. Hehre and J. A. Pople, Self-consistent molecular-orbital methods. IX. an extended Gaussian-type basis for molecular-orbital studies of organic molecules, *J. Chem. Phys.*, 1971, **54**, 724–728.

38 M. J. Frisch, *et al.*, *Gaussian 09*, Gaussian, Inc., Wallingford CT, 2016.

